CORROSION SCIENCE AND TECHNOLOGY, Vol.31, No.4(2002), pp.305~310

Combined Effect of Calcium and Silicon on the Seaside Corrosion Property of Weathering Steel

Woo Taek Jeong and Kyoo Young Kim

Pohang University of Science and Technology, Center for Advanced Aerospace Materials
San 31 Hyoja-Dong, Pohang 790-784 Korea

The combined effect of Ca and Si on the corrosion properties of weathering steel was investigated by pH measurement, AC impedance testing, and cyclic corrosion and atmospheric exposure test. Although the short-term test results of pH measurement and AC impedance test showed that high Si content indicated an adverse effect on the corrosion resistance, the long-term test results of cyclic corrosion and atmospheric exposure revealed that the Ca-modified weathering steel containing 0.62% Si had the best corrosion resistance due to increase of compactness of rust layer.

Keywords : *weathering steel, Ca-modification, Si effect, formation of α-FeOOH*

1. Introduction

The corrosion resistance of the weathering steel is mainly dependent upon the formation of dense and stable α-FeOOH in the rust. It demonstrates excellent protective properties against atmospheric corrosion.[1-3] However, it takes a long time (in excess of 10 years) to develop this protective rust layer, which forms with difficulty in marine environments containing Cl^-; moreover, β-FeOOH forms easily in such environment.[4] Since β-FeOOH is less dense than other types of rust due to its structure, corrosive anions such as Cl^- or H_2O molecules easily penetrate the rust layer and continue to corrode weathering steel.[5]

It has been also reported that the addition of Ca in weathering steel can induce strong alkalinity in water film and promote the formation of α-FeOOH.[6] The addition of Ca to weathering steel forms complex inclusions containing CaO and CaS which can dissolve completely in the thin water film. Due to dissolution of complex inclusions, the alkalinity of thin water film increases, and protective rust layer composed of α-FeOOH forms. However, it has been speculated that Si in the weathering steel can form complex oxides of $CaO_x \cdot SiO_2$ or $CaO \cdot Al_2O_3 \cdot 2SiO_2$, which may decrease the beneficial effect of Ca addition on the corrosion property due to the acidic nature of SiO_2.[7]

In this investigation, The combined effect of Ca and Si on the corrosion resistance was evaluated by short-term tests of pH measurement and AC impedance test and long-term tests of cyclic corrosion and atmospheric exposure tests. The rust structure was also analyzed by Raman spectroscopy and Mossbauer spectroscopy.

2. Experimental

Two different groups of test specimens with and without Si were prepared by fixing compositions of other major alloying elements. Table 1 lists the compositions of the test specimens used for this study. The corrosion properties of the specimens were evaluated by inclusion analysis, pH measurement, AC impedance test, cyclic corrosion test, and actual atmospheric exposure test.

The inclusion presented in the steel was analyzed to verify the existence of Ca-and Si-compounds. Morphology of these inclusions was observed by scanning electron microscopy (SEM) and the elemental analysis was performed by energy dispersive spectroscopy (EDS). The AC impedance test was performed to evaluate the effect of Ca and Si on the corrosion resistance. A two-electrode

Table 1. Chemical compositions of tested specimens(wt%)

No.	C	Si	Mn	P	S	Cu	Al	Ni	Ca (ppm)	O (ppm)	N (ppm)
SI1	0.098	-	0.97	0.014	0.008	0.405	0.028	0.49	11	41	37
SI2	0.094	-	0.99	0.013	0.009	0.406	0.033	0.97	20	50	38
SI3	0.097	-	0.99	0.014	0.008	0.400	0.034	0.50	57	39	60
SI4	0.107	0.226	1.06	0.015	0.009	0.430	0.049	1.03	60	56	49
SI5	0.099	0.385	0.98	0.013	0.010	0.395	0.038	0.97	64	45	33
SI6	0.107	0.620	0.99	0.013	0.010	0.401	0.039	0.99	68	33	32

cell configuration was employed. A pair of two identical steel sheets (0.2 mm W × 3 mm L) was mounted in an epoxy resin 0.2 mm apart in parallel. A thin electrolyte film is covered on the surface of the specimen electrode in the cell and 0.1M and 0.01M NaCl were used as electrolyte. The impedance was measured in a frequency range of 10k Hz to 10m Hz with an amplitude of 10mV. The pH-measurement of the water film on the steel was carried out to investigate the dissolution of complex inclusions containing Ca-compounds. To measure the pH value of the water film covering the steel, a micro pH electrode was employed. Distilled water and 0.1M NaCl solution were used as the water film and pH-measurement was carried out every 10 minutes over 2 hours.

Cyclic corrosion test was carried out in a corrosion chamber which would simulate a marine environment with various conditions of wet and dry cycles and a Cl^- deposition rate of 0.8 mdd ($mg/dm^2/day$). After 480 cycles of testing, analyses of the rust layer included examination of rust morphology using scanning electron microscopy (SEM), and phase identification using Raman spectroscopy. Mossbauer spectroscopy was also employed to identify different oxyhydroxide phases formed on weathering steel. For atmospheric exposure test, test specimens were exposed at Wolpo beach near Pohang city in Korea. After the atmospheric exposure test, the rust formed on the steel specimens was removed and the corrosion depth was determined.

3. Results and discussion

3.1 Analysis of inclusions

Addition of a small amount of Ca results in formation of calcium oxide or calcium sulfide. These oxide and

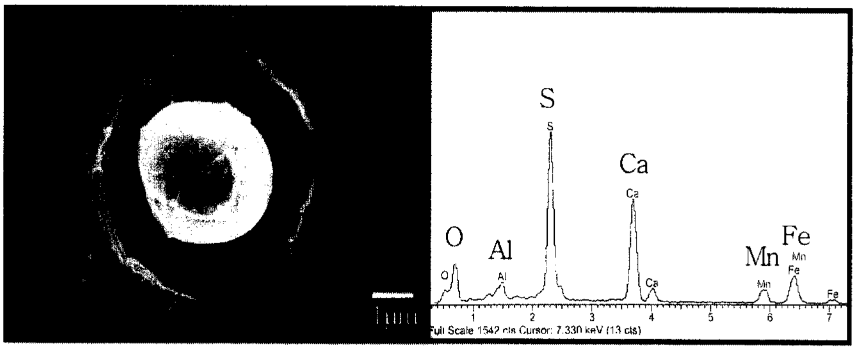

(a)

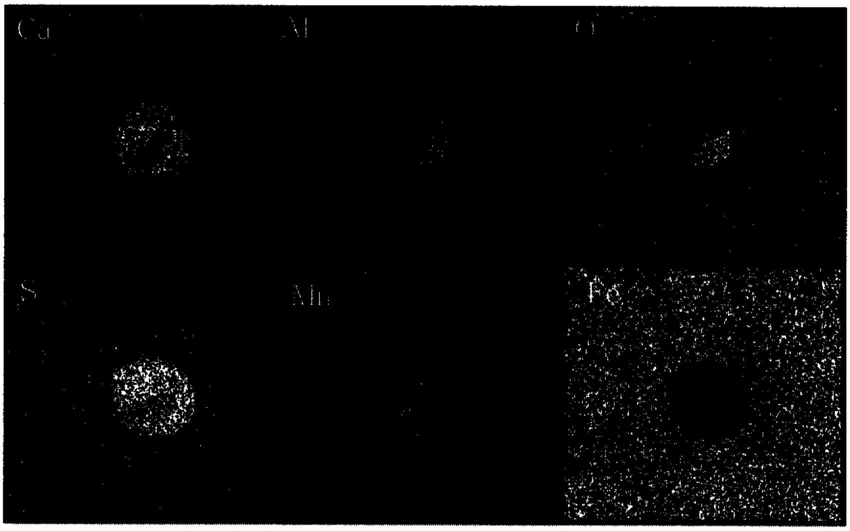

(b)

Fig. 1. (a) Typical morphology of an inclusion formed in Ca-modified steel, SI5 (64ppm Ca-0.39%Si) and EDS spectra. (b) Elemental analysis by EPMA on an inclusion observed from SI5.

sulfide usually form complex inclusions of Ca-Al-Mn-O-S during the steel making process. Fig. 1 shows a typical morphology and an elemental analysis of the Ca-containing inclusion formed in SI5 containing 64ppmCa-0.39%Si. No inclusion containing Si was observed until about 0.4% Si content. However, SI6 containing 68ppmCa-0.62%Si seldom showed inclusions containing Si. Even though inclusions containing Si were observed from SI6, only a few inclusions contained Si, but most inclusions did not contain Si at all.

3.2 pH measurement

Fig. 2 shows the trend of pH change in thin water films covered on the Ca-modified weathering steels with and without Si. In distilled water film, regardless of the presence of Si, the specimens containing Ca more than 50 ppm increased pH value with time, whereas the specimens containing Ca less than 20 ppm decreased. The increasing rate of pH slowed down as the Si content in the Ca-modified steel increased. However, pH value increased with time up to 0.4% Si. Besides, the pH value for SI6 containing 0.62% Si maintained nearly a constant pH value after initial increase. In 0.1M NaCl solution, regardless of Si content in the steel, the pH values of all the specimens decreased with time. This may be due to hydrolysis of Fe^{2+} in the Cl^- ion containing solution. However, the decreasing rate of pH value depends mainly upon the amount of Ca content in the steel. The CaO and CaS in Ca-modified weathering steel dissolved easily in water film, and increased its pH value in distilled water or slowed the decreasing rate of the pH value in the 0.1M NaCl solution. It has been speculated that Si can form complex oxides of $CaO_x \cdot SiO_2$ or $CaO \cdot Al_2O_3 \cdot 2SiO_2$ which will impede the beneficial effect of Ca addition on the corrosion property due to the acidic nature of SiO_2.[7] However, because the formation free energies of CaO and Al_2O_3 are much lower than that of SiO_2,[9] Si does not

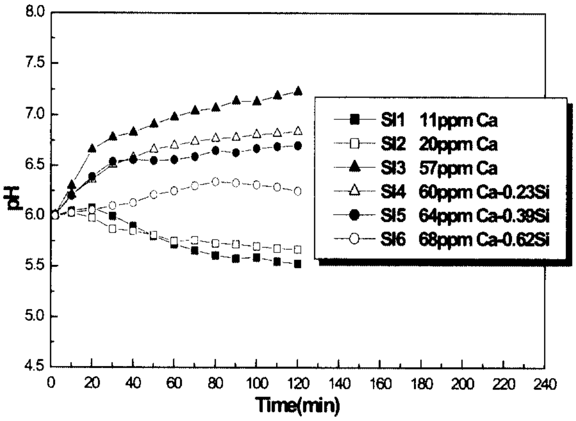

(a)

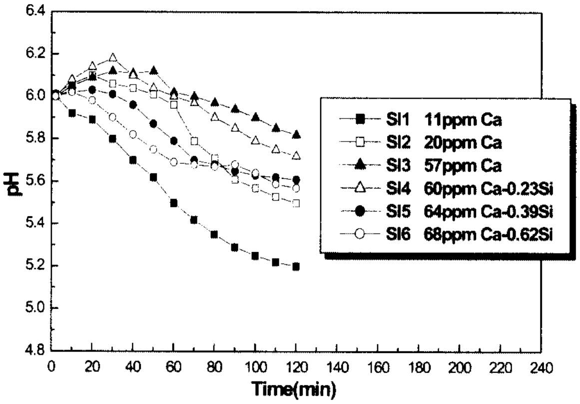

(b)

Fig. 2. Change in pH value of thin water film measured for 2 hours at room temperature using a micro-pH electrode (a) in distilled water (b) in a 0.1M NaCl solution. The water film thickness was 2mm.

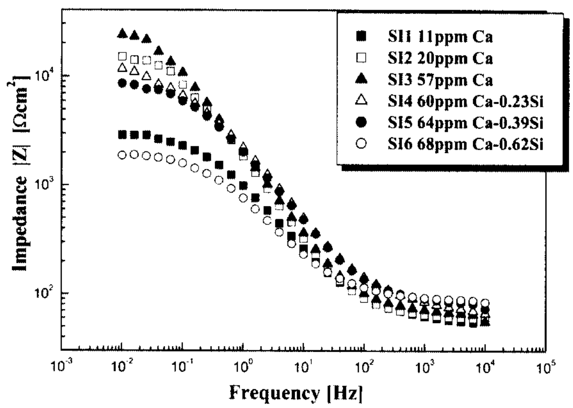

(a)

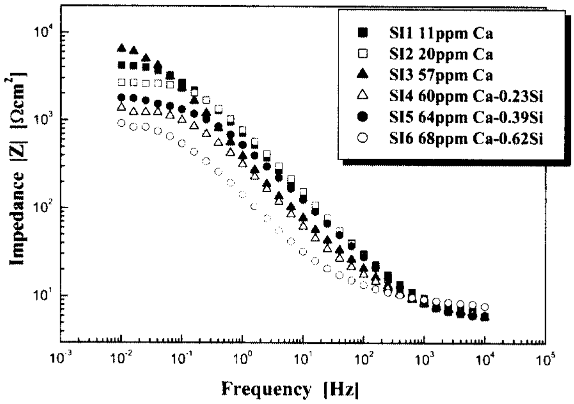

(b)

Fig. 3. Bode plots of AC impedance data for the specimens covered with a thin water film of (a) 0.01M NaCl solution (b) 0.01M NaCl solution

have any opportunity to form an oxide and it remains in the steel as a solid solution. It is clearly proved that the Ca-modified weathering steel containing Si no more than 0.6% does not form complex oxides of $CaO_x \cdot SiO_2$ or $CaO \cdot Al_2O_3 \cdot 2SiO_2$.

3.3 AC impedance test

AC impedance test was performed to evaluate the effect of Ca and Si on the corrosion property of the weathering steel covered with a thin water film. Fig. 3(a) shows Bode plot representing the results of AC impedance measurement in the 0.01M NaCl solution. The value of polarization resistance is the highest for SI3 (57ppm Ca with no Si), but the lowest for SI6 (68ppm Ca-0.62%Si). These results imply that the polarization resistance can be increased with addition of Ca, whereas it can be decreased with addition of Si. However, with optimum amount of Ca, Si content up to 0.4% may not give a harmful effect. Fig. 3(b) shows the AC impedance results measured in 0.1M NaCl solution. Although the values of polarization resistance shift downward with increase in NaCl concentration, the order of the polarization resistance value is similar to the results observed from 0.01M NaCl solution. The short-term test results of pH measurement and AC impedance test show that, with optimum level of Ca content (50-70 ppm), Si content up to 0.4% in the Ca-modified weathering steel did not give a harmful effect on the corrosion resistance, but Si content more than 0.62% may give an adverse effect on the corrosion resistance.

3.4 Cyclic corrosion test simulating a marine environment

In order to understand the effect of Ca and Si content on the structure and constituent of rust layer, corrosion test was performed in a cyclic corrosion chamber simulating a marine environment with various conditions of wet and dry cycles. Through observation of the surface morphology of the rust layer after 480 cycles, it was realized that the rust layer consisted of two layers of an outer loose layer and inner dense one. The outer layer has a loose structure consisting of small particles, while the inner layer has very dense structure with fine particles. Therefore, it can be assumed that the corrosion resistance of weathering steel is mainly dependent upon the structural nature of inner layer rather than that of outer layer. Fig. 4 shows the result of Raman spectroscopic analysis on the rust layer formed on SI5 (64ppm Ca and 0.39%Si). The rust layer composed of dark inner layer and brighter outer layer. It was identified that α-FeOOH mainly was present in the inner layer and β-FeOOH mainly in the outer layer. From this analysis, it is clear that α-FeOOH is responsible for the compact structure of the inner rust layer

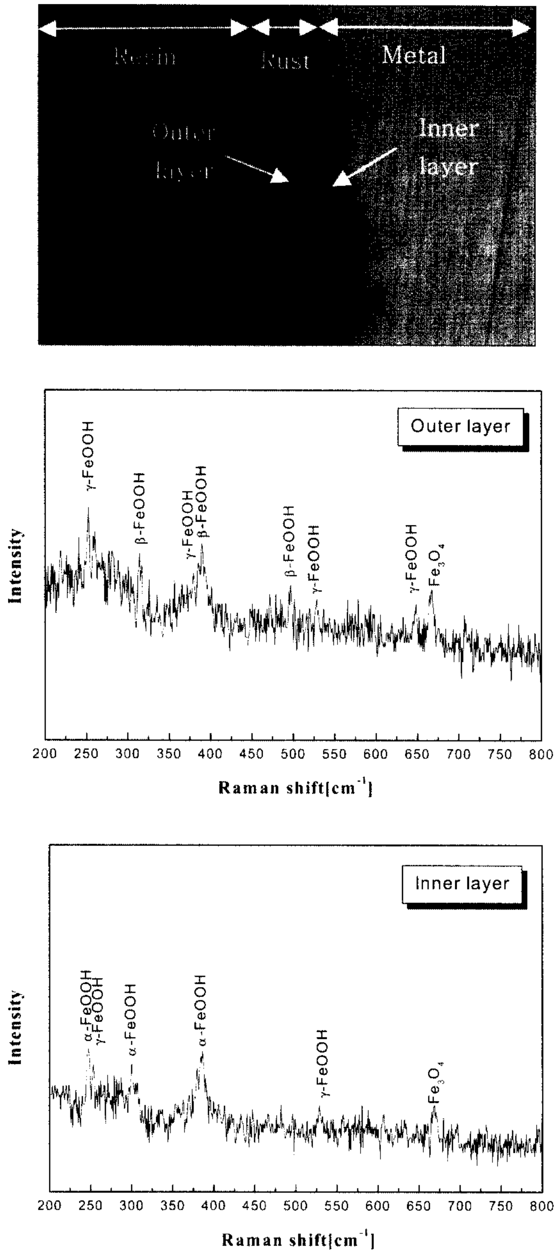

Fig. 4. Image and phase identification by Raman analysis across the rust layer formed on the SI5 specimen over 480 cycles in the cyclic corrosion tester.

Fig. 5 compares the cross-sectional morphologies of rust layers in terms of content of Ca and Si. From the morphological analysis on the rust layer formed by cyclic corrosion test (Fig. 5), it is understood that, regardless of Si content, the rust structure becomes dense and compact as the amount of Ca increases. As listed in Table 3, the micro-hardness value of the rust layer increased as the amount of Ca and Si increased. In fact, SI6 had the highest

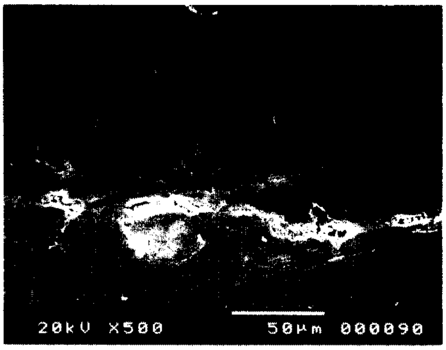

(a) Specimen SI1 (11ppmCa)

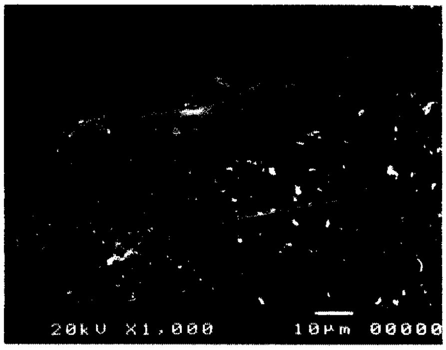

(b) Specimen SI3 (57ppmCa)

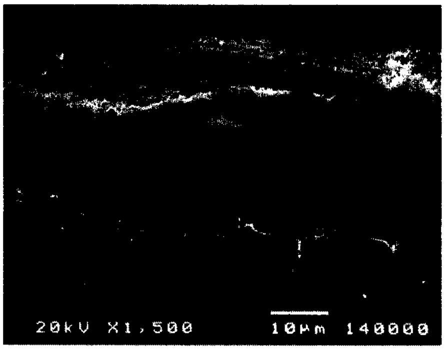

(c) Specimen SI4 (60ppmCa-0.23Si)

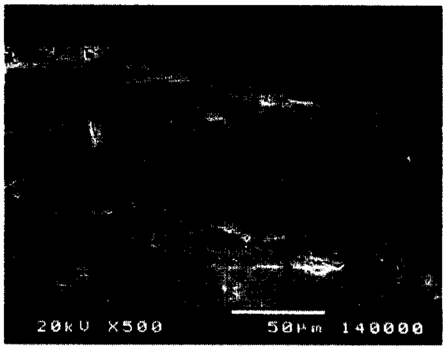

(d) Specimen SI6 (68ppmCa-0.62Si)

Fig. 5. Cross-sectional morphologies of rust layers formed on the surface of specimens corroded during 480 cycles in the cyclic corrosion tester.

Table 2. Result of Mössbauer spectroscopic analysis on corrosion products obtained after 240 and 480 cycles.

Corrosion products	240 cycles					480 cycles				
	SI1	SI3	SI4	SI5	SI6	SI1	SI3	SI4	SI5	SI6
α-FeOOH	13	23	19	20	17	19	34	23	22	21
β-+γ-FeOOH	61	57	64	67	65	53	50	54	53	61
Fe_3O_4	26	20	17	13	18	28	16	23	25	17

Table 3. Hardness values of the rust layers formed on the steel specimens after cyclic corrosion and exposure tests.

Specimen	Cyclic Corrosion Test	Exposure Test
SI1 (11ppm Ca)	135.2	222.9
SI2 (20ppm Ca)	164.3	229.2
SI3 (57ppm Ca)	188.7	242.1
SI4 (60ppm Ca - 0.23 Si)	141.4	199.1
SI5 (64ppm Ca - 0.39 Si)	183.9	233.3
SI6 (68ppm Ca - 0.62 Si)	223.5	266.1

hardness value for the rust layers formed after cyclic corrosion test of 480 cyclies. Mossbauer spectroscopy was used to understand the effect of Ca and Si content on the constituent of the rust layer. Table 2 lists the volume fraction of corrosion products formed on the steel surface after 240 and 480 cycles. As the corrosion cycles and Ca content are increased, formation of α-FeOOH increases while that of β-FeOOH and γ-FeOOH decreases. It clearly suggests that rust layer consisted of β-FeOOH and γ-FeOOH transfers to α-FeOOH by long-term corrosion process or alkalization of corrosion environment.

3.5 Atmospheric exposure test

Fig. 6 shows the change in corrosion depth of the Ca-modified weathering steels during exposure test at Wolpo site. A plain carbon steel (0.13C-0.55Si-1.46Mn-0.02P-0.005S-0.014Cu-0.013Ni-0.02Cr-0.045Al) was included in the test set for comparison. All the data definitely demonstrate that addition of Ca improves corrosion resistance of the weathering steel. The Ca-modified steels containing Si showed better corrosion resistances than those without Si. In particular, although all the laboratory

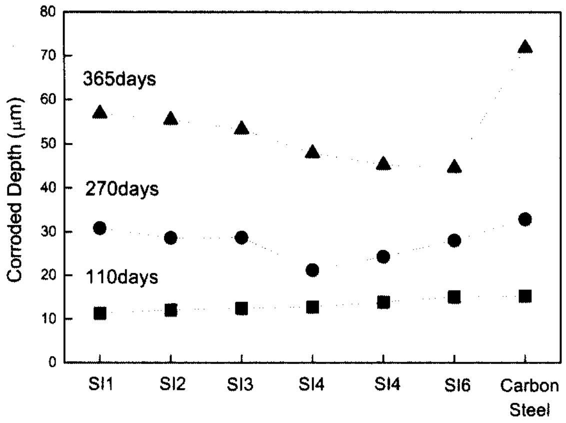

Fig. 6. Change in corrosion depth of the steel specimens during atmospheric exposure in a marine environment.

tests including pH measurement, and AC impedance indicated that Si content of 0.62% gave an adverse effect on the corrosion property of Ca-modified weathering steel, the actual exposure test result showed that SI6 containing 0.62% Si had the best corrosion resistance. This result suggests that, if Ca content in a range of 50~70 ppm is added, addition of a small amount of Si is not harmful but may be beneficial for corrosion resistance. The hardness data of specimen exposed seaside corrosion environment for 12 months is listed in Table 3. In general, for the Ca-modified specimens without Si, the hardness value increased with increase in Ca content, and for the Ca-modified specimens with Si, the hardness value increased with increase in Si content. Surprisingly, the hardness value of SI6 containing the highest amount of Si(0.62%) was the highest. These hardness data strongly indicate that the corrosion resistance of the Ca-modified steel can be improved with addition of optimum amount of Si by formation of rust layer with compact structure. According to the data obtained from this investigation, it can be suggested that the corrosion resistance of the Ca-modified weathering steel containing Si can be improved by the following 3 different mechanisms: 1) Alkalization of the thin water film by dissolution of the Ca-containing inclusions. 2) Formation of a dense and protective α-FeOOH in the rust by repeated wet/dry cycles. 3) Additional densification of the rust structure by modification of Si. Therefore, it can be clearly stated that, if the weathering steel contains an optimum level of Ca, the presence of a small amount of Si will be beneficial for corrosion resistance. However, a further study is required to understand the specific role of Si for compactness or densification of the rust structure.

4. Conclusions

1) Ca-addition in a range of 50-70 ppm increased the pH value of the water film, promoted α-FeOOH formation in the rust, and improved overall corrosion resistance of steel.

2) The short-term test results of pH measurement and AC impedance test show that, with optimum level of Ca content (50-70 ppm), Si content up to 0.4% in the Ca-modified weathering steel did not give a harmful effect on the corrosion resistance, but Si content more than 0.62% may give an adverse effect on the corrosion resistance.

3) The long-term test results of cyclic corrosion and atmospheric exposure revealed that rust structure became dense and compact as amount of Ca and Si increased. Especially the Ca-modified weathering steel containing 0.62% Si had the best corrosion resistance by formation of rust layer with compact structure.

References

1. T. Misawa, K. Asam, K. Hashimoto, and S. Shimodaira , *Corr. Sci.*, **14**, 279 (1974).
2. M. Yamashita, H. Nagano, T. Misawa, and H. E. Townsend, *ISIJ International*, **38**, 285 (1998).
3. M. Yamashita, H. Miyuki, H. Nagano, and T. Misawa, *Tetsu-to-Hagane*, **83**, 36 (1997).
4. A. Usami, *CAMP-ISIJ*, **9**, 482 (1996).
5. H. Miyuki, M.Yamashita; M. Fujiwara, and T. Misawa, *Zairyo-to-Kankyo*, **47**, 186 (1998).
6. M. Yamamoto, H. Kihira, A. Usami, K. Tanabe, K. Masuda, and T. Tsuzuki, *Tetsu-to-Hagane*, **84**, 36 (1998)
7. Patent, Jp. No.H07-242993, (1995).
8. M. Yamashita H. Miyuki, Y. Matsuda, H. Nagano, and T. Misawa, *Corros. Sci.*, **36**, 283 (1994).
9. I. Barin, in *Thermochemical Data of Pure Substances*, VCH Publishers, New York, (1989).